STRAIN MEASUREMENT IN WOOD USING A DIGITAL IMAGE CORRELATION TECHNIQUE

Audrey G. Zink

Assistant Professor
Wood Science and Forest Products
Virginia Polytechnic Institute and State University
Blacksburg, VA 24061-0323

Robert W. Davidson

Professor Emeritus
Wood Products Engineering
SUNY-CESF
Syracuse, NY 13210

and

Robert B. Hanna

Professor and Director
Center for Ultrastructure Studies
Wood Products Engineering
SUNY-CESF
Syracuse, NY 13210

ABSTRACT

The suitability of the Digital Image Correlation Technique (DICT) for full-size test specimens of wood and wood-based composites was evaluated in this study. The technique utilizes pairs of digitized video images of undeformed and deformed test specimens and an image correlation computer routine to measure the displacements of any or all points on the surface of the test specimen. New methods for image acquisition and image correlation were developed and evaluated in this study.

Evaluation and calibration were performed using an aluminum alloy block for comparison and axial compression of small, clear specimens of wood and in accordance with ASTM D143-83 (1986a). Comparison of strain measurements obtained using an independent measurement technique and strain obtained with the DICT showed close agreement. Utilizing DICT for full-field strain distributions through an increasing load series revealed progressive failure development in the wood specimens, the eventual failure mode, and a shift in strain concentrations during load application.

Keywords: Strain measurement, image analysis, mechanical testing.

INTRODUCTION

Full-field experimental measurement of the distribution of strain in wood has traditionally been tedious and difficult due, in part, to equipment limitations. Previously brittle coatings, photoelasticity, moiré methods, and laser speckle interferometry have been investigated. Each of these methods requires surface treatments and/or modifications that change the mechanical properties on a local level or that require complex, intensive, and expensive preparation and equipment. Because of the complexity and expense of these methods, examination of only a few specimens is economically possible. Dial gauges, electrical strain gauges, and linear variable differential transducers have been the conventional devices for measuring point-wise strain in a wood specimen or structure. These devices measure strain

over a very limited gauge length and as a result, cannot be used for full-field measurement.

Recently, an application of computer vision has developed that can be used as a full-field method in experimental mechanics. The Digital Image Correlation Technique (DICT) relies on a mathematical correlation of digital images of the surface of test specimens acquired during mechanical testing. Because of widespread interest and the potential demonstrated with small specimens of wood in previous work by the authors and colleagues (Choi 1990; Choi et al. 1991; Zink 1992), the modifications required to the video microscopy approach of Choi et al. (1991) for application to full-size wood test specimens are outlined in this paper.

BACKGROUND

It was shown by Peters and Ranson (1982) and Sutton et al. (1983) that the use of white light illumination of a random, black and white pattern made it possible to obtain strain measurements with optical techniques in conjunction with a digital computer. In this research they developed extensive mathematical and experimental techniques for cross-correlating a reference image with a stored image for application in experimental mechanics. The cross-correlation technique is similar to area correlation in pattern recognition methodology. The cross-correlation of two functions is used to indicate the relative amount of agreement between the two functions for various degrees of shifting. In the case of experimental mechanics, the displacement imposed on the test object during mechanical loading is measured as the degree of shifting of the light intensity patterns as found by the cross-correlation criterion. Since its development, DICT has been applied to a range of testing conditions including rigid body mechanics (Sutton et al. 1983), dynamics (Peters and Ranson 1982), fluid mechanics (He et al. 1984), biomechanics (Ranson et al. 1986), and most recently, fracture mechanics (Luo et al. 1994) and micromechanics (Vendroux 1994).

The application of DICT and video microscopy for the measurement of full-field displacements and strains in small specimens of wood and paper was investigated recently by Choi (1990) and Choi et al. (1991). It was shown in this application that DICT could be a fast, simple, and accurate method when applied to very small specimens of wood (1 mm × 1 mm × 4 mm in size) and paper. These researchers determined that the strain fields on the surface of the small compression specimens exhibited a large variation in magnitude and sign even under uniform loading, that high strain concentration areas developed prior to reaching a proportional limit in the stress-strain behavior, and that differences in the strain measurements between load steps represented strain redistribution during relaxation. It was determined that the nonuniform strain fields were closely related to the surface morphology of the wood. On the microscopic scale, the strain concentration locations were determined by the size, location, and arrangement of the rays and the mechanical properties of the wood cell elements.

Zink (1992) applied the image correlation technique to measure the strain distribution in double overlap wood joints. The distribution of strain along the gluelines was measured using scaled versions of full-size wood truss connections, and finite element models were constructed of these joints. The measurement matrix was arranged on the test specimens so that the measurement points corresponded with the finite element node locations in the model of the joints. Very good agreement was observed between the experimentally measured strain distributions and the model values.

EXPERIMENTAL PROCEDURES

Digital Image Correlation Technique (DICT)

Equipment setup.—In the past, the equipment used to acquire and digitize the video images was a CCD video camera and an image digitizer board in a personal computer, and in the case of video microscopy, direct access through the microscope (Choi et al. 1991). A

new method for image acquisition was investigated in this project for full-size specimens that utilized a 35-mm Nikon camera, a 55-mm macro lens for specimen magnification, and white light specimen illumination to acquire the images on black and white film during the testing. In general, image acquisition requires transporting the video camera, peripherals, and computer into the testing lab for digitization while the testing is in progress or direct access through a video microscope for very small specimens. The photographic film approach examined in this study offers the advantage of portability for full-size specimens and field application, and it minimizes handling of sensitive video and image capture equipment.

A typical test setup is illustrated in Fig. 1. The choice of camera and lens depends on the magnification required; however high-quality lenses must be used to ensure accurate measurements. A 35-mm camera and 55-mm lens format was used in this study due to its widespread accessibility and popularity. Other larger formats could provide a larger field of view and could be just as suitable. The camera must be mounted on a stable tripod that is insensitive to floor vibrations, and care must be taken to ensure that the image plane of the camera is exactly parallel with the test specimen surface. The f-stop on the camera should be chosen to optimize surface contrast through the combination of illumination and magnification. The white light sources used in this study were 500W photo flood lamps placed at 45° angles to the specimen surface. For smaller test specimens, any uniform, unchanging light source can be used that provides adequate specimen illumination—for example, fluorescent tubes or fiber optic illuminators. Typical flash attachments that come with still cameras did not provide uniform, unchanging illumination of the specimen and are not recommended. In any test situation, care must be taken to eliminate illumination variation from other sources such as room lights or natural light through windows.

The film used in this study was black and white TMax, ASA 100, and the exposure time was 1/30 second. This film was used because of the high stability of the film emulsion and its high degree of resolution. High resolution, stable films have been developed recently and others would probably prove as suitable. In this study, all images from a testing series were recorded on a single film strip. This must be done to ensure that all test images in a series are chemically processed exactly the same way and guarantee that there are no artifacts introduced in image acquisition through the film processing.

Once the test specimen images were acquired with the still camera, the film images were then placed in film holder on a light box and advanced through the load series. Using lower projection of light through the film, the images were sequentially transmitted to the video camera, which was rigidly mounted above the film holder on the light box for digitization. A 55-mm macro lens was attached to the video camera through a standard C-mount adaptor. The macro lens provides focus and enlargement of the photographic image. In this study, magnification factors ranged from $1.5 \times$ to $3 \times$. Other camera lenses can be used, depending on the range of magnification required. A frame alignment device must be used to guarantee consistent placement of the film images throughout the testing series. In this study, consistency of placement was controlled through the test series by lining up an object placed near the test specimen in the images with marks placed on the film holder. Commercial devices are now available that advance film at consistent distances without image shift due to rotation or misalignment, through a tractor-feed mechanism similar to that used in the 35-mm still cameras.

Slight misalignment of the film images through the series can be tolerated when using iterative searching algorithms because all points in the image will be shifted in equal magnitude and direction. Any rigid body translation can be identified and subtracted from the image displacements using the correlation computer program as described in the following section.
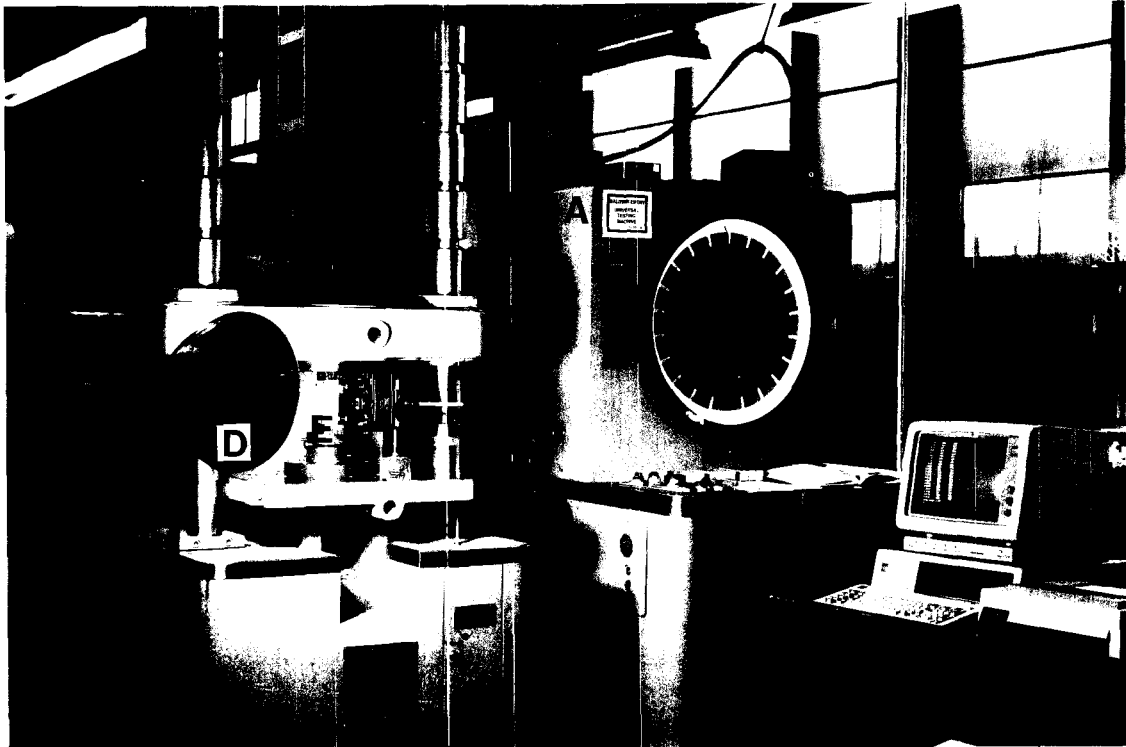
FIG. 1. Laboratory test setup for the Digital Image Correlation Technique: A = Mechanical testing machine, B = Personal computer used for load and LVDT data acquisition, C = 35-mm camera used for photographic image acquisition, D = Photoflood light, and E = Compression test specimen.

Using the programs developed in this and previous work (Choi et al. 1991; Zink 1992), misalignment of ± 10 pixels was the tolerance range for rigid body motion due to film image placement; however, this range can be adjusted to meet specific conditions. The film images were digitized using a Panasonic WV-CD50 CCD camera and a Coreco Oculus-200 image digitizer board in an IBM personal computer. The matrix resolution for this system was 480 × 512 pixels. The image and measurement resolution is dependent on the magnification factors resulting from image magnification. Currently, there are many high resolution CCD video cameras and digitizing systems available.

Correlation analysis. — The digitization process represents the continuous light intensity patterns of the recorded images in a discrete

numeric form. Because a pixel in undeformed coordinates may relocate to positions between pixels in deformed coordinates, an interpolation of gray levels between pixels is needed to represent the original continuous pattern. Through the interpolation of gray levels between pixels, measurement of displacements less than 1 pixel is possible. Several interpolation methods exist; however, a bilinear scheme has been found to be the most reliable and efficient (Chu 1982; Sutton et al. 1983). As a result, a bilinear interpolation scheme was used in this study and the previous video microscopy work of Choi et al. (1991). In this method, a hyperbolic paraboloid expression is used to estimate the intensity distribution for any square set of four sample points. The paraboloid is defined by a linear equation, and the piece-wise bilinear function interpolates

adjacent four pixel neighborhood boundaries to provide intensity values between pixels for sub-pixel resolution.

The digitized intensity pattern after deformation is related to the digitized, interpolated intensity pattern recorded before deformation through the object deformations. A mathematical correlation of the two images to determine image differences allows for determination of object displacement. The image correlation program compares subsets of digitized light intensity vales of subregions around selected pixel locations in the undeformed images with subregions of the same size in the deformed image.

The correlation analysis utilizes selected subregions to find the values of six unknown parameters that minimize the correlation function, C. C is a nonlinear function dependent on the subregion size and the unknown parameters and must be unique for each selected pixel location. In this study, the correlation function was the sum of the squares of the differences of the light intensity values of the subregions in the pairs of images and is a "least squares" correlation to measure how well the subsets match. It is written:

$$C(u, v, \delta u/\delta x, \delta u/\delta y, \delta v/\delta x, \delta v/\delta y) =$$
$$= \sum_{M} [A(x, y) - B(x', y')]^2 \qquad (1)$$

where u and v are the displacements for the subset centers in the x and y direction, respectively, A(x, y) is the gray level value at coordinate (x, y) in the deformed image, B(x', y') is the gray level value at point (x', y') in the undeformed image, and M is the subset of interest chosen from the digital images.

In this study, the subregion, M, used for the pattern matching was 20 × 20 pixels in size and centered around the selected measurement points. This size subregion was chosen to minimize the effects of local wood structure deviations, minimize image distortion, reduce correlation time, and obtain a pattern that was statistically different from its neighbors. Other subregion sizes may be appropriate for other

investigations as determined through experimentation.

The coordinates (x, y) and (x', y') are related by the deformation that occurred between acquisition of the two images as imposed by the mechanical loading. If the motion of the object relative to the camera is parallel to the image plane and the deformations are small, the images are related by

$$x' = x + u + (\delta u/\delta x)(\Delta x) + (\delta u/\delta y)(\Delta y) \quad (2)$$

and

$$y' = y + v + (\delta v/\delta x)(\Delta x) + (\delta v/\delta y)(\Delta y) \quad (3)$$

where u and v are the displacements for the subset centers in the x and y directions, respectively. The terms Δx and Δy are the distances from the subset center to the point (x, y).

Correlation of the images is obtained by determining the values for the six unknown parameters: u, v, $\delta u/\delta x$, $\delta u/\delta y$, $\delta v/\delta x$, and $\delta v/\delta y$ which minimize the correlation coefficient, C. Minimization of functions, or optimization as this procedure is often called, is a very large area of numerical research. Various schemes exist in the literature on image correlation. In general, a coarse-fine search technique for determining the best fit value has been used. This procedure requires a very large number of calculations and is very computationally intense, especially for full-size specimens or fieldwork. The video microscopy of Choi et al. (1991) utilized the traditional coarse-fine iterative procedure.

A new method for obtaining the pattern matching was evaluated in this study: the quasi-Newton method for approximation of polynomials. This method was used to provide the successive approximations of the initial guesses of the six unknown deformation parameters. A two-parameter model was iterated until all values were within the tolerance limits. The values of the six unknown parameters that minimize the correlation function, C—Eq. (1) are returned as the best approximations to the six deformation parameters. This method provided convergence with fewer calculations needed and as such, greatly decreased the com-

putational time required for full-size specimens. In this study, the correlation analyses were performed on a time-share IBM 3090 mainframe processer. With a coarse-fine iterative procedure for convergence, measurement of the displacement of one grid point required 9 seconds CPU time, 34.25 seconds wall clock time. Only 0.3912 seconds of CPU time and 1.56 seconds wall clock time were required per grid point with the quasi-Newton method. For a small number of grid points, this time savings is not significant, but for full-size specimens, hundreds of measurements must be made and the time saving becomes substantial. The displacements due to external loading as measured with the image correlation technique can be determined with a computer-image measurement matrix of any desired size; however, the measurement points should be located in the central portion of the image to minimize edge effects and curvature of the field.

Calibration and evaluation. —Extensive evaluation and calibration procedures were carried out on the experimental equipment and image correlation computer program. Testing to determine system noise levels involved acquisition of images at several time intervals and determination of the differences of the digital gray values between these images. A carbon speckle pattern as described in a following section was applied to the surface of an aluminum alloy block, the block was placed on the table of the testing machine, and images of the entire surface were acquired over time. No load was applied to the specimen during this experiment, none of the equipment was moved, and the light was constant throughout the experiment. Four 20 × 20 subsets of digital gray values were chosen at random locations on the surface of the aluminum block for each time interval and were compared to the reference image acquired at time = 0. It was observed that there were no apparent strains in the 60 min allowed for this testing.

Accuracy and precision estimates were determined by comparing strains obtained with the vision system and the strains as measured with a compressometer, which had been carefully calibrated to a secondary standard with known accuracy. The standard definitions are applied for accuracy and precision (Holman 1984) as follows: the accuracy of the vision system was defined as the maximum deviation of the readings from this known input, and the precision was defined as the maximum deviation of several readings from the mean of those readings. Calibration tests were conducted on an aluminum alloy block to minimize any effects from material structure and because it is a typical isotropic, homogeneous, elastic material.

The electronic device used for the calibration was a Daytronics DS190V linear variable differential transducer (LVDT). The LVDT was carefully calibrated just prior to testing using a T63R1 Starrett micrometer head. The accuracy of the micrometer was found to be $\pm 1.27 \times 10^{-3}$ mm. The precision of the micrometer was $\pm 1.27 \times 10^{-3}$ mm. The full scale of the micrometer was 5.08 mm. The accuracy and precision of both the micrometer and the LVDT in terms of percent of full-scale reading were found to be $\pm 0.025\%$. Axial strain was measured between two points, and the gauge length was the same for both techniques. The test was replicated ten times. It was determined that the accuracy of the computer vision system was $\pm 0.025\%$ of a full-scale reading of 5.08 mm, and coincidentally, the precision was also $\pm 0.025\%$. The standard deviation of the displacements was ± 0.021 pixels. The magnification factors were: 1 in. on the test specimen equaled 190 pixels in the x-direction and 144 pixels in the y-direction of the computer image. At this magnification, displacement measurement resolution was ± 0.02 pixels or 0.0028 mm ($\sim 1/10,000$ inch) in the y-direction and 0.0035 mm in the x-direction. Figure 2 is the calibration curve for the aluminum calibration block. The vertical bars associated with each data point represent the standard deviation at each data point from ten replications of the testing.

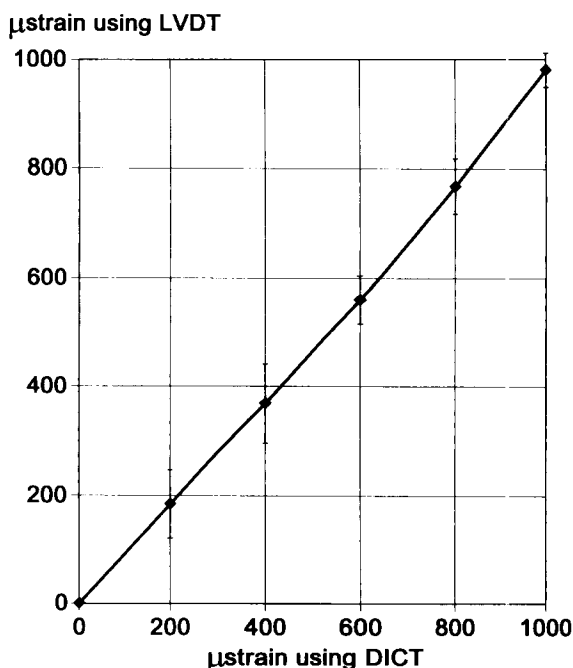Distortion from out-of-plane effects was minimized by working with low magnifica-

μstrain using LVDT

Fig. 2. Calibration curve for aluminum alloy calibration block for μstrains measured with the Digital Image Correlation Technique and an LVDT.

tions (<3×), a high-quality lens with a large depth of field, and specimen-to-lens working distances of >400 mm. Sutton et al. (1990) have determined that magnification of <5× and a distance from the camera lens plane to the object of >400 mm are sufficient to reduce to an acceptable range any distortion from out-of-plane movement of the specimen. They determined that at these levels, any noise that appears in the displacement fields is from sources other than out-of-plane effects.

Strain distribution measurement. —The normal strains (ϵ_{xx} and ϵ_{yy}) between each measurement point can be calculated as the change in distance between the points in the x-direction or y-direction divided by the original distance between the points ($\Delta L_x/L_x$ and $\Delta L_y/L_y$) using the displacements of each point as measured with the image technique. The shear strain (ϵ_{xy}) can be calculated as the change in angle between adjacent sides of an elementary block defined by four measurement points as

this block was distorted under shearing stresses. The change in angle can be determined using the displacements of each of the four points as measured with the image technique.

In this study, a finite difference method that utilized a forward difference scheme was employed for the strain field calculations. The average standard deviation in the strain measurements was ±270 μstrain. No filtering or noise smoothing of the strain data was employed in this study; however, Sutton et al. (1991) and Lukasiewicz et al. (1993) have found that noise can be successfully filtered out of the strain fields using smoothing algorithms.

Specimen preparation

Fabrication. —Measurement of the displacements using the image correlation technique is not limited by the materials, the testing environments, or the testing duration. The only requirement is visual access to the desired surface during the loading and consistent, uniform specimen illumination. For laboratory evaluation of the applicability to full-size wood specimens, thirty small, clear test specimens of sugar pine (Pinus lambertiana) were prepared in this study in accordance with ASTM D143-83 Standard Methods of Testing Small Clear Specimens of Timber (1986a). The test specimens were 25.4 × 25.4 mm in cross section and 101.6 mm along the grain. The average initial moisture content was 8.5% on a dry weight basis. A similar-sized aluminum alloy block was employed for comparison and evaluation purposes. Hydrogen peroxide was used to clean and dull the shiny aluminum surface.

Carbon speckle application. —Because the technique relies on a comparison of discrete light intensity patterns obtained before and during deformation to obtain the shift of the images, a unique, random intensity pattern is required on the surface of observation. Homogeneous metals, composites, and wood specimens, in general, do not provide the required unique, sharp contrast patterns. In addition, the surfaces of the test specimens must

not create glare such as a shiny piece of metal and must be free of any dirt or dust.

In this study, the unique contrast pattern was created on the surface of the aluminum alloy block and wood specimens with a light speckle of carbon particles such as those found in photocopy toner cartridges. Unused toner should be applied because used toner particles will be electrically charged and may not stick to the test specimens. These toner particles are distinctly black in hue and contain carbon black and chrome III pigments. The particles were sifted through a screen held about 150 mm (6 in.) above the surface of the specimen and allowed to scatter across the specimen surface via room air currents. Heat was applied to the carbon particles using a heat lamp. The particles melted and flowed into the test specimen structure after 10 min in an air temperature of approximately 70 C. The specimens were then allowed to cool. During the cooling process, the particles solidified and, in the case of the wood specimen, became tightly anchored to the wood structure. Figure 3 is an example of the desired coverage rate.

The advantages of this particular speckle pattern are that it does not mask the underlying wood structure and it does not modify the material properties of the test specimen in any manner. This speckling pattern provided adequate coverage as demonstrated with the small specimens of wood and paper in the previous study (Choi et al. 1991); however, extra care must be taken to control the coverage rate and speckle pattern with this technique when applied to full-size specimens. For specimens larger than laboratory sizes, this technique does not provide ample contrast enhancement. Other techniques such as paint speckles or ink dots can be used.

Moisture conditioning.—To avoid any erroneous displacements due to dimensional change from changing moisture content of hygroscopic materials, test specimens should be conditioned to approximate the equilibrium moisture content that will be obtained in the testing laboratory, or testing should be conducted in a controlled environment. The wood evaluation specimens in this study were conditioned using an Amino-Aire Humidity-Temperature Control chamber. The specimens were weighed periodically until no weight change was noticeable and were kept in the chamber at constant conditions until just prior to testing. The average moisture content of the specimens at test was 12% as determined by ASMT Standard D2016-83 Method A, Oven-dry Method (1986b).

RESULTS AND DISCUSSION

Because it is possible with the image correlation technique to measure displacements for as little as one point and as many as thousands of points for full-field analysis, there are many diverse and useful methods for data representation. The techniques vary from a simple table of the displacement or strain values, to a stress-strain plot using as few as two points, to lines of measurement points on the specimen, to full-field strain plots using a measurement matrix of points.

Material structure

The sensitivity of the technique to the material structure can be illustrated with a series of measurement gauges that consist of lines of measurement points as seen in Fig. 4. Figure 4A is a plot of μstrain parallel-to-the-load along five gauge lines on an aluminum block; and Fig. 4B is the μstrain parallel-to-the-load plot along five gauge lines on a wood block. The load applied to these blocks was a uniform, uniaxial load in accordance with ASTM D143-83 (1986a). The specimens were 25.4 × 25.4 mm in cross section and 101.6 mm along the length. There were five measurement points along each line in the y-direction at gauge lengths of 20 mm, and the lines were spaced 5 mm apart.

It can be seen in Fig. 4A that the μstrain along the five measurement lines in the aluminum block was fairly uniform, with little variation along and among the measurement lines. The range of μstrain values varied from 1,800 to 2,000 μstrain. Based on the homo-

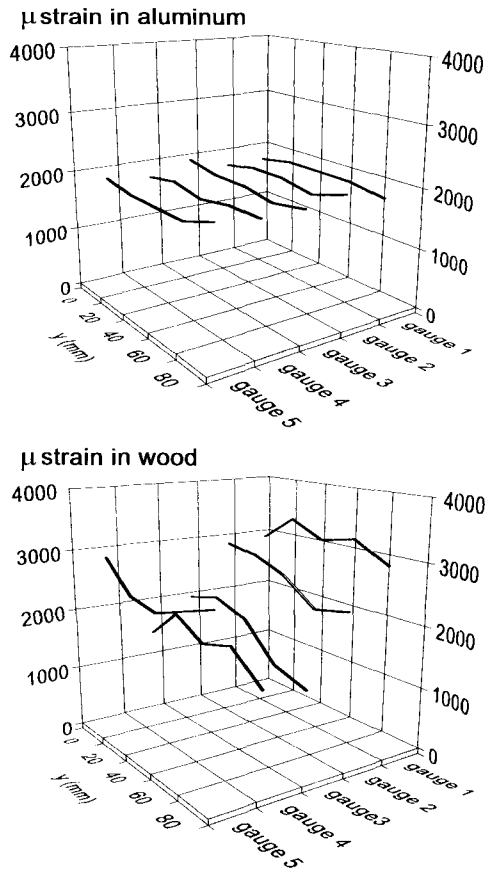FIG. 3.   Photograph of a representative speckle pattern (4×).

μ strain in aluminum

A

μ strain in wood

B

FIG. 4.   μstrain parallel to the load along five gauge lines using DICT A: Aluminum Alloy Block B: Wood Block.

FIG. 5.   Load/Deflection plot and image acquisition points for compression test specimen #3.

geneity on a macroscopic scale for aluminum, the strain at several points on the surface would be expected to be fairly uniform in magnitude for a uniform, uniaxial load. Examination of Fig. 4B indicates that the heterogeneity of wood does affect the strain values in full-size specimens even under a uniform, uniaxial load. The two measurement lines closest to the edges of the specimen exhibit the highest values, and there is variation along and among all lines of data. The range of the μstrain values for the wood specimen was 1,250–2,950 μstrain. The nonuniformity of the strains in the wood specimens was observed on the surface of the small compression specimens as tested in previous studies (Choi et al. 1991) and is reflective of
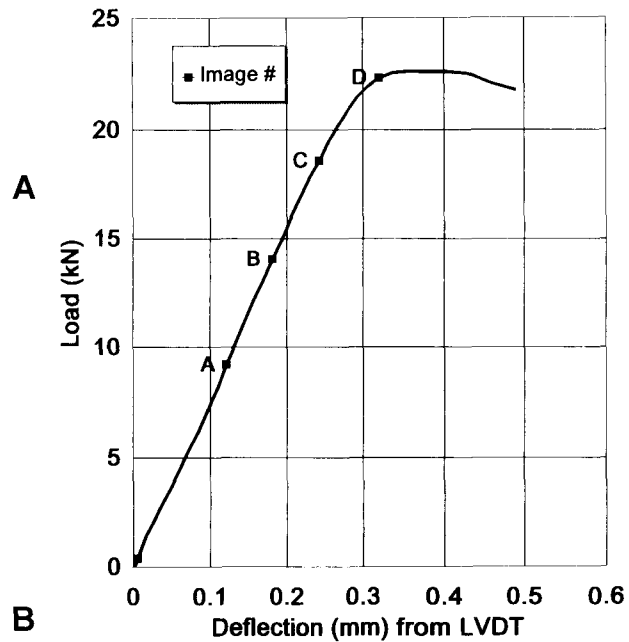
the wood morphology even in full-size specimens.

Full-field strain distributions through a load series

Figures 5, 6, 7, and 8 illustrate examples of the type of information that can be gained through the application of DICT for full-field analysis of wood in compression through an increasing load series. The loads at which the strain distributions were measured are indicated in Fig. 5—Load/Deflection as steps A, B, C, and D. Figure 6 is the full-field contour plot of the strains perpendicular to the load ($\mu\epsilon_{xx}$), and Fig. 7 is the full-field strain contour plot parallel to the load ($\mu\epsilon_{yy}$) for the same wood compression specimen as in Fig. 6. These isostrain contour plots were calculated from displacements measured with the image correlation method using the image acquired at a slight preload as the reference image. As a result, the strain values in each figure represent the strain that accumulated from the onset of that initial load up to the load at which the
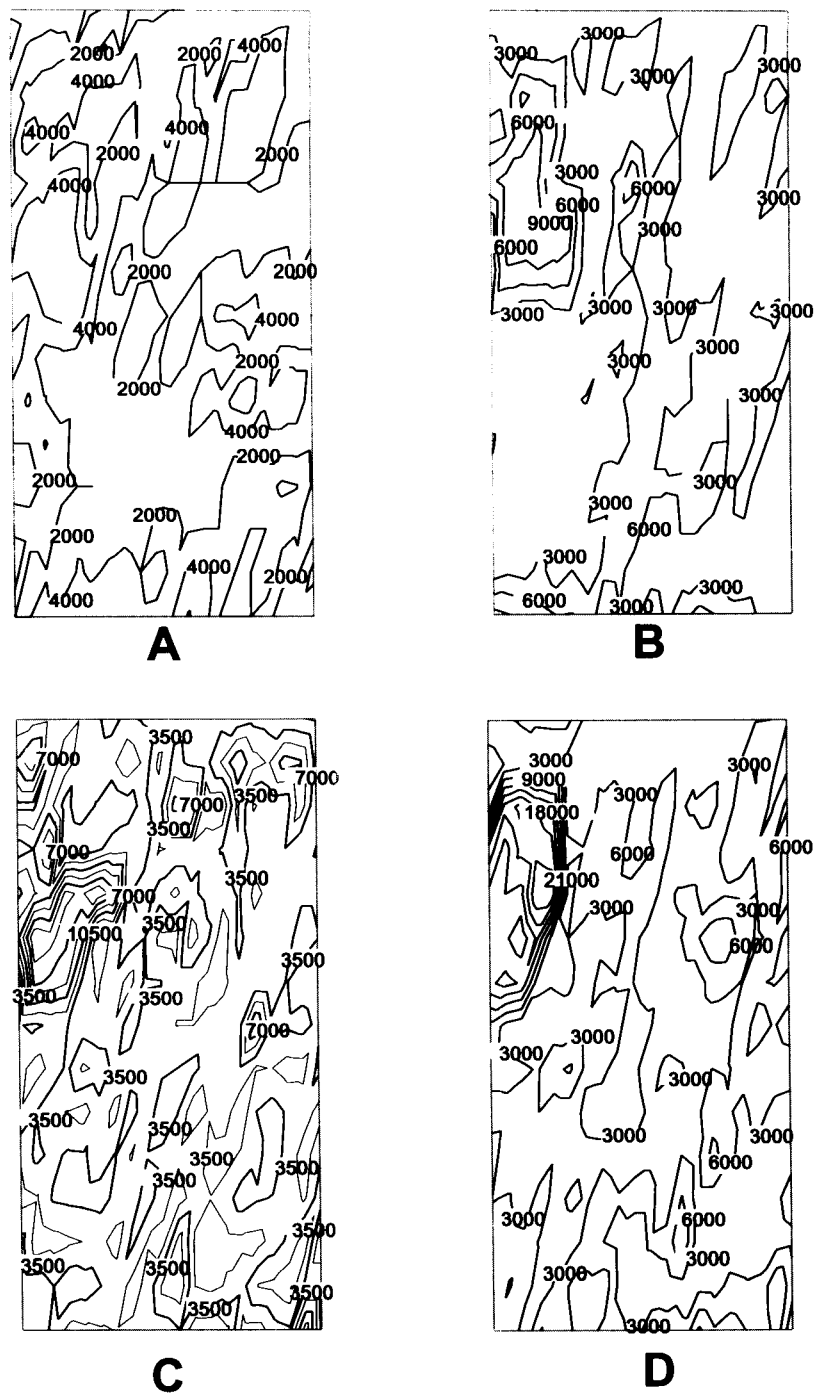
FIG. 6.   Full-field μstrain perpendicular to the load for wood compression test Specimen #3; A: Load = 9.21 kN, B: Load = 14.05 kN, C: Load = 18.60 kN, D: Load = 22.32 kN.
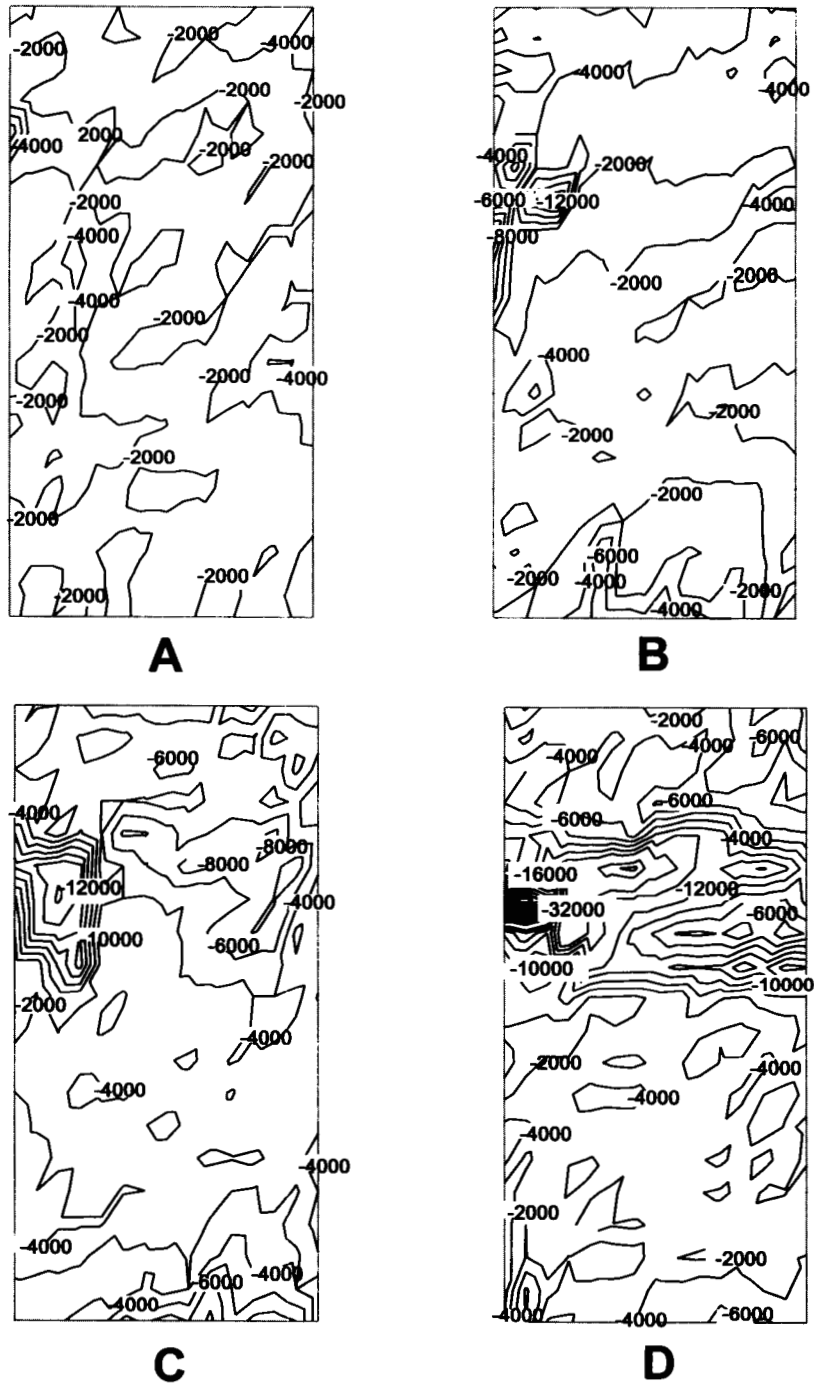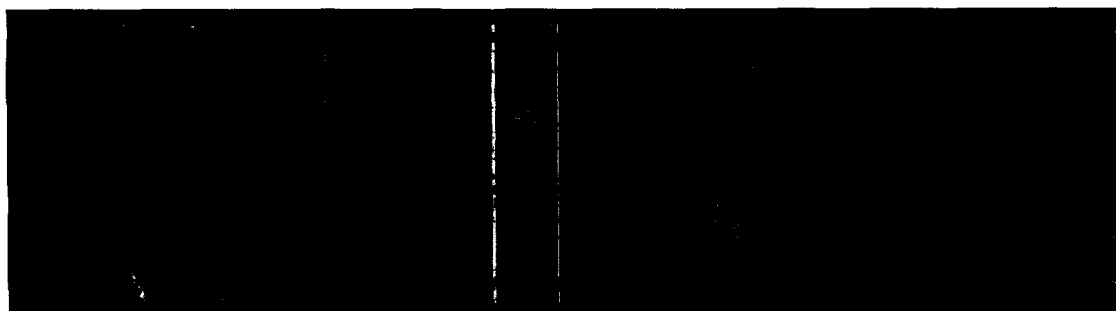
FIG. 7. Full-field μstrain parallel to the load for wood compression test Specimen #3; A: Load = 9.21 kN, B: Load = 14.05 kN, C: Load = 18.60 kN, D: Load = 22.32 kN.

FIG. 8. Photograph of failed wood compression specimen #3.

images were acquired. The measurement matrix consisted of 15 points perpendicular to the load (x-direction) and 20 points parallel to the load (y-direction). Each of the points was placed at 20 pixel intervals on the computer image for corresponding gauge lengths of 1.33 mm in the x-direction and 3.85 mm in the y-direction on the test specimen. The computer-image measurement grid of 300 points was located in the central portion of the image to minimize edge effects and is the surface area between the two vertical lines as seen in Fig. 8.

Examination of Figs. 6A, B, C, & D—$\mu\epsilon_{xx}$ indicates that under uniform compression load parallel to the grain, there are tension strains perpendicular to the grain even at low load levels that eventually become highly localized through the increasing load series. This type of information provides experimental confirmation of the Poisson effect in wood on a full-field basis and it is now possible to calculate Poisson ratios for entire test specimens.

Examination of Figs. 7A, B, C, & D indicates that the distribution of strain parallel to the load—$\mu\epsilon_{yy}$ is not as homogeneous as might be expected from a uniform compression load applied parallel to the grain. The strains begin to accumulate in a highly localized region even prior to reaching a proportional limit in load. As observed with very small wood specimens by Choi et al. (1991), the unique microscopic features of the wood elements are responsible for the inhomogeneous nature of the strain fields in full-size specimens, and the previously held assumption of a uniform strain distri-

bution is not valid for the specimens examined in this study.

A comparison of Fig. 8, which is a photograph of the failed specimen in question, and the strain plots in Figs. 6 and 7 indicates that the location of highest strain on both the strain plots parallel to the load and perpendicular to the load ($\mu\epsilon_{xx}$ and $\mu\epsilon_{yy}$) exactly corresponds to the location of visible failure lines on the test specimen.

SUMMARY AND CONCLUSIONS

The image correlation technique was shown to be an accurate, simple, and versatile method of measuring strain distributions in full-size specimens of wood and wood-based composites. The technique is noncontact and is not limited by the size or nature of the specimen. The modifications required for scale-up from video microscopy (Choi et al. 1991) to full-size specimens of wood and composites involved: 1.) making the image acquisition system portable through using a still camera, such as a 35-mm camera format, and specimen illumination with white-light photofloods, to acquire film images of the test specimens during loading; 2.) digitizing the film images by lower projection of light through the 35-mm film images, image magnification with a video camera and enlargement lens, and digitization of the light intensity values using an image capture board in a personal computer connected to the video camera; 3.) improving the correlation computer program to increase the

computational turnaround time through a quasi-Newton pattern matching scheme.

With the strains distributions as measured with the image correlation technique, it is possible to obtain an early indication of strain concentration areas, correlate these areas with structure, and predict eventual failure location. The full-field strain distributions at several stages of load revealed progressive failure development, the eventual failure mode, and a shift in strain concentrations during load application. Full-field strain distributions can also be used to confirm or disprove existing theories and assumptions about wood and wood-based products. Because widespread application of full-field experimental methods in wood mechanics has not occurred in the past, it has only been possible to speculate on the actual strain distribution during load application.

ACKNOWLEDGMENTS

REFERENCES

ASTM. 1986a. Standard methods of testing small clear specimens of timber. Standard D143-83. American Society for Testing and Materials, Philadelphia, PA.

————. 1986b. Ovendry method. Standard D2016-83, Method A. American Society for Testing and Materials, Philadelphia, PA.

CHOI, D. 1990. Failure initiation and propagation in wood in relation to its structure. Ph.D. dissertation, State University of New York, Syracuse, NY.

————, J. L. THORPE, AND R. B. HANNA. 1991. Image analysis to measure strain in wood and paper. Wood Sci. Technol. 25:251–262.

CHU, T. C. 1982. Digital image correlation method in experimental mechanics. Ph.D. dissertation, University of South Carolina, Columbia, SC.

HE, Z. H., M. A. SUTTON, W. R. RANSON, AND W. H. PETERS. 1984. Two-dimensional fluid-velocity measurements by use of digital speckle correlation techniques. Exp. Mech. 24(2):117–121.

HOLMAN, J. P. 1984. Experimental methods for engineers. 4th ed. McGraw-Hill Book Co., New York, NY.

LUKASIEWICZ, S. A., M. STANUSZEK, AND J. A. CZYZ. 1993. Filtering of the experimental data in plane stress and strain fields. Exp. Mech. 33(2):139–147.

LUO, P. F., Y. J. CHAO, AND M. A. SUTTON. 1994. Experimental evaluation of J-integral using both in-plane deformations and caustics obtained from out-of-plane displacements. Pages 248–253 *in* Proc. 1994 SEM Spring Conference on Experimental Mechanics, June 1994, Baltimore, MD.

PETERS, W. H., AND W. F. RANSON. 1982. Digital imaging techniques in experimental stress analysis. Optical Eng. 21(3):427–431.

RANSON, W. F., D. M. WALER, AND J. B. CAULFIELD. 1986. Biomechanics *in* Computer vision in engineering mechanics, a discussion paper for the NSF Workshop on Solid Mechanics Related to Paper, August, 1986, Blue Mountain Lake, New York.

SUTTON, M. A., W. J. WOLTERS, W. H. PETERS, W. F. RANSON, AND S. R. MCNEILL. 1983. Determination of displacements using an improved digital correlation method. Image Vision Comput. 1(3):133–139.

————, T. L. CHAE, J. L. TURNER, AND H. A. BRUCK. 1990. Development of a computer vision methodology for the analysis of surface deformations in magnified images. ASTM STP 1094, MiCon 90, 109–132. American Society for Testing and Materials, Philadelphia, PA.

————, J. L. TURNER, H. A. BRUCK, AND T. A. CHAE. 1991. Full-field representation of discretely sampled surface deformation for displacement and strain analysis. Exp. Mech. 31(2):168–177.

VENDROUX, G. 1994. Scanning tunneling microscopy in micromechanics investigations. Ph.D. thesis, California Institute of Technology, Pasadena, CA.

ZINK, A. G. 1992. The influence of overlap length on the stress distribution and strength of a bonded wood double lap joint. Ph.D. dissertation, SUNY-CESF, Syracuse, NY.